RESEARCH PAPER

Macrophage stimulating protein promotes liver metastases of small cell lung cancer cells by affecting the organ microenvironment

**Seidai Sato · Masaki Hanibuchi · Takuya Kuramoto · Nodoka Yamamori ·
Hisatsugu Goto · Hirohisa Ogawa · Atsushi Mitsuhashi · Trung The Van ·
Soji Kakiuchi · Shin-ichi Akiyama · Yasuhiko Nishioka · Saburo Sone**

Abstract The organ microenvironment significantly affects the processes of cancer metastasis. Elucidating the molecular mechanisms of interaction between tumor cells and the organ microenvironment is crucial for the development of effective therapeutic strategies to eradicate cancer metastases. Macrophage stimulating protein (MSP), an activator of macrophages, regulates a pleiotropic array of effects, including proliferation, cellular motility, invasiveness, angiogenesis, and resistance to anoikis. However, the role of MSP in cancer metastasis is still largely unknown. In this study, the action of MSP on the production of metastases was determined in a multiple-organ metastasis model. The murine MSP gene was transfected into two human SCLC cell lines, SBC-5 and H1048, to establish transfectants secreting biologically active MSP. MSP gene transduction did not affect cell proliferation and motility in vitro. Intravenously inoculated MSP transfectants produced significantly larger numbers of liver metastases than parental cells or vector control clones, while there were no significant differences in bone or lung metastases among them. Immunohistochemical analyses of liver metastases revealed that tumor-associated microvessel density and tumor-infiltrating macrophages were significantly increased in lesions produced by MSP transfectants. MSP could stimulate the migration of murine macrophages and endothelial cells in vitro. Consequently, MSP may be one of the major determinants that affects the properties of tumor stroma and that produces a permissive microenvironment to promote cancer metastasis.

Keywords Small cell lung cancer · Liver metastasis · Macrophage stimulating protein · Organ microenvironment

Abbreviations

MSP	Macrophage stimulating protein
RON	The recepteur d'origine nantais
SCLC	Small cell lung cancer
NK	Natural killer
SCID	Severe combined immunodeficient
MEM	Minimum essential medium
FBS	Fetal bovine serum
GFP	Green fluorescent protein
RT-PCR	Reverse transcription-polymerase chain reaction
GAPDH	Glyceraldehyde 3-phosphate dehydrogenase
HGFA	Hepatocyte growth factor activator
MTT	3-(4,5-dimethylthiazol-2-yl)-2,5-diphenyl tetrazolium
TAM	Tumor-associated macrophage

S. Sato · M. Hanibuchi · N. Yamamori · H. Goto ·
A. Mitsuhashi · Y. Nishioka (✉) · S. Sone
Department of Respiratory Medicine and Rheumatology,
Institute of Health Biosciences, The University of Tokushima
Graduate School, 3-8-15, Kuramoto-cho, Tokushima
770-8503, Japan
e-mail: yasuhiko@clin.med.tokushima-u.ac.jp

T. Kuramoto · T. T. Van · S. Kakiuchi · S. Akiyama · S. Sone
Department of Medical Oncology, Institute of Health
Biosciences, The University of Tokushima Graduate School,
3-8-15, Kuramoto-cho, Tokushima 770-8503, Japan

H. Ogawa
Department of Molecular and Environmental Pathology,
Institute of Health Biosciences, The University of Tokushima
Graduate School, 3-8-15, Kuramoto-cho, Tokushima
770-8503, Japan

Introduction

Lung cancer is one of the major causes of malignancy-related death worldwide, and its incidence is increasing in

many counties. The manifestation of distant metastases to multiple organs is the most devastating complication and the main reason for poor prognosis in lung cancer. Unfortunately, more than 70 % of lung cancer patients have advanced stage disease at the time of diagnosis [1]. Although intensive efforts have been made to treat lung cancer, the eradication of lung cancer metastases is still a very challenging issue. Therefore, elucidating the molecular and biological mechanisms of lung cancer metastasis is essential to develop more effective therapeutic strategies.

Macrophage stimulating protein (MSP) was originally identified as a serum protein that elicited macrophage chemotaxis and activation [2]. MSP is secreted as an inactive single-chain precursor, pro-MSP [3–5], which becomes active after proteolytic cleavage by proteases [5, 6]. The recepteur d'origine nantais (RON) is a receptor tyrosine kinase with significant homology to c-Met, a potent proto-oncogene [7], and the only known ligand for RON is MSP [5, 8]. Upon binding by MSP, RON is activated via autophosphorylation within its kinase catalytic domain, resulting in a pleiotropic array of effects, including cellular motility, adhesion, proliferation, tubular morphogenesis, and apoptosis [9, 10]. Recently, much attention has been paid to the role of MSP in tumor progression and metastasis [11–13]. In a spontaneous metastasis model of mouse mammary tumors, MSP promoted distant metastases to various organs, especially to bone [12]. MSP was also reported to be a candidate gene that may affect bone tropism of human small cell lung cancer (SCLC) because the expression of MSP was up-regulated in bone metastatic lesions [13]. However, the role of MSP on cancer metastasis is not fully elucidated.

The goal of this study was to determine whether MSP affect the properties of tumor stroma and host microenvironment to promote cancer metastasis. As we sought to generate a model in which mouse MSP would be secreted and act on mouse organ environment, mouse MSP gene was overexpressed in human SCLC cell lines. Then, we examined the effect of MSP overexpression on the production of experimental metastases in natural killer (NK)-cell depleted severe combined immunodeficient (SCID) mouse model.

Materials and methods

Cell lines

The human SCLC cell line, SBC-5 [14] was kindly provided by Drs. M. Tanimoto and K. Kiura (Okayama University, Okayama, Japan). The human SCLC cell line, H1048 was purchased from American Type Culture Collection (Manassas, VA). Human adenocarcinoma cell line,

ACC-LC319 was kindly provided by Dr. T. Takahashi (Nagoya University, Nagoya, Japan) and its highly metastatic subline, ACC-LC319/bone2 was established as described previously [15]. Human adenocarcinoma cell line, PC14PE6, a highly metastatic variant of PC14, was kindly provided by Dr. I. J. Fidler (M.D. Anderson Cancer Center, Houston, TX), and human adenocarcinoma cell line, A549 was purchased from IBL Japan (Ibaraki, Japan). Human lung squamous cell carcinoma cell line, H226 was kindly provided by Dr. J. D. Minna (University of Texas Southwestern Medical Center, Dallas, TX). All cells were maintained in Eagle's minimum essential medium (MEM) and RPMI1640 medium respectively, each supplemented with 10 % heat-inactivated fetal bovine serum (FBS), penicillin (100 U/ml), and streptomycin (50 μg/ml). The murine macrophage-like cell line, RAW264.7, and the murine endothelial cell line, MS1, were purchased from American Type Culture Collection (Manassas, VA). A potent retrovirus packaging cell line, PLAT-E [16], was kindly provided by Dr. K. Yasutomo (The University of Tokushima, Tokushima, Japan). RAW264.7, MS1, and PLAT-E cells were cultured in Dulbecco's modified MEM supplemented with 10 % FBS, penicillin (100 U/ml), and streptomycin (50 μg/ml). All cells were maintained at 37 °C in a humidified atmosphere of 5 % CO_2 in air.

Reagents

Anti-mouse interleukin-2 receptor β-chain monoclonal antibody, TM-β1 (IgG2b), was supplied by Drs. M. Miyasaka and T. Tanaka (Osaka University, Osaka, Japan) [17]. Anti-mouse MSP antibody was purchased from Santa Cruz Biotechnology (Santa Cruz, CA).

MSP gene transduction

Replication-defective mouse stem cell viruses, pMIG which expressed green fluorescent protein (GFP) only, and pMIG-MSP which expressed MSP and GFP, were kindly provided by Dr. A. L. Welm (University of Utah, Salt Lake City, UT). The PLAT-E packaging cell line was transfected with pMIG or pMIG-MSP using Fugene 6 (Roche, Indianapolis, IN). SBC-5 and H1048 cells were infected with each viral supernatant. Then, 8 μg/ml of polybrene (Sigma, St. Louis, MO) was added. The mixture was spun at 2,500 rpm for 60 min at room temperature and then incubated for 72 h. Infected GFP-positive cells were sorted by flow cytometry (JSAN cell sorter; Bay bioscience, Kobe, Japan). After culturing the initial sorted population, GFP-positive cells comprised more than 85 % of the whole cell population. One clone and a vector control clone were established in each cell line, which were designated as SBC-5-MSP, SBC-5-Vector and H1048-MSP, H1048-Vector, respectively.

Reverse transcription-polymerase chain reaction (RT-PCR)

The expression of mouse MSP mRNA was determined by RT-PCR. Total cellular RNA and RNA from liver metastatic lesions were isolated using RNeasy Mini Kit (Qiagen, Valencia, CA) according to the manufacturer's protocols. Total RNA was reversely transcribed using a TaqMan® RNA-to-CT™ 2-Step kit (Applied Biosystems, Foster City, CA). The primers of mouse MSP and β-actin were as follows: MSP: 5′-GCT ACA CCA CAG ACC CGA AT-3′ and 5′-GGT ATT GGT TGT GCC TCG AT-3′; β-actin: 5′-AAG AGA GGC ATC CTC ACC CT-3′ and 5′-TAC ATG GCT GGG GTG TTG AA-3′. PCR was performed using Ampli Taq Gold (Applied Biosystems, Foster City, CA). Bands were visualized by ethidium bromide staining. PCR amplification of cDNA was performed under the following conditions: 30 cycles, 30 s at 94 °C; 30 s at 58 °C; 30 s at 72 °C. Before the first cycle, a denaturation step for 2 min at 94 °C was included, and after 30 cycles, the extension was prolonged for 7 min at 72 °C [18]. PCR products were analyzed by 1.5 % agarose gel electrophoresis and visualized by ethidium bromide staining with UV light.

Quantitative reverse transcription-PCR

Quantitative real-time RT-PCR for mouse cell lines and tissues were performed using SYBER Premix EX Taq system (TAKARA) and Applied Biosystems StemOnePlus (ABI). Amplified signals were confirmed to be single band by gel electrophoresis and were normalized to the levels of glyceraldehyde 3-phosphate dehydrogenase (GAPDH). Data was analyzed using StepOneSoftware (ABI). The PCR primer sequences used are as follows : mouse GAPDH, 5′-CAA CTA CAT GGT CTA CAT GTTC-3′ (forward) and 5′-CGC CAG TAG ACT CCA CGAC-3′ (reverse); mouse hepatocyte growth factor activator (HGFA), 5′-TGA GGG ACC CCA AAG TGA GA-3′ (forward) and 5′-GCA CTT CCC TCA GAG GTA CA-3′ (reverse); mouse MSP, 5′-AGT TAA GGA ACC TGT TAC AC-3′ (forward) and 5′-ACC ATG GCT GCT CAT GTT GT-3′ (reverse); mouse RON, 5′-ATT GAA GAG GGT GTC GAA TA-3′ (forward) and 5′-TCA AAG GGA AGT AGT GGC AA-3′ (reverse). The expression of human RON and human β-actin were measured by quantitative real-time RT-PCR analysis on an ABI 7,700 Sequence Detection system (Applied Biosystems, Foster City, CA) with the following commercially available sets of primers and fluorogenic probes (TaqMan_Gene Expression Assays products): RON, Hs00234013_m1; β-actin, Hs99999903_m1.The quantitative RT-PCR experiments were done in triplicate, and the relative expression levels were calculated based on the comparative Ct method.

Western blotting

After incubation for 48 h, the supernatants of each cell line and homogenized mouse tissue samples were then harvested and their protein concentrations were determined using a protein assay (Bio Rad, Hercules, CA). For Western blot analysis, 30 μg of total proteins were resolved by SDS-PAGE (Invitrogen Life Technologies, Carlsbad, CA) and proteins were then transferred to PVDF membranes (Atto, Tokyo, Japan). After washing three times, membranes were incubated with Blocking One (Nacalai Tesque, Kyoto, Japan) for 1 h at room temperature, then incubated for 1 h at room temperature with anti-mouse MSP antibody (1:1,000 dilution; Santa Cruz, CA), anti-human and mouse RON antibody (1:200 dilution; Santa Cruz, CA) or anti-mouse pRONβ antibody (1:200 dilution; Santa Cruz, CA). Membranes were then incubated for 30 min at room temperature with species-specific horseradish peroxidase conjugated secondary antibodies. Immunoreactive bands were visualized using enhanced chemiluminescent substrate (Pierce, Rockford, IL).

Cell proliferation assay

Cell proliferation was measured using the 3-(4,5-dimethylthiazol-2-yl)-2,5-diphenyl tetrazolium (MTT) dye reduction method [19]. Tumor cells (2×10^3 cells/100 μl/well) were seeded into each well of a 96-well plate and incubated for 24–96 h. After incubation, 50 μl of stock MTT solution (2 mg/ml; Sigma, St. Louis, MO) was added to all wells, and cells were then further incubated for 2 h at 37 °C. Media containing the MTT solution was removed, and 100 μl of DMSO was added. Absorbance was measured with an MTP-32 Microplate Reader (Corona Electric, Ibaragi, Japan) at test and reference wavelengths of 550 and 630 nm, respectively.

Transwell migration assay

Human SCLC cells (SBC-5, H1048) and their subclones were incubated for 24 h in MEM with 10 % FBS, then were incubated for 48 h in MEM with 0.1 % FBS. Thereafter, culture supernatants were harvested and added to the bottom wells of a 24-well Cell Culture Insert (8.0 μm pore size; Becton–Dickinson, NJ). RAW264.7 cells or MS1 cells (1×10^5 cells/well) were seeded in the top wells and cultured in MEM with 0.1 % FBS for 17 h or 6 h, respectively. After incubation, cells that remained in the top chamber were removed with a cotton swab, migrated cells were fixed, and DNA was labeled with

Hoechst33342 (Dojindo Laboratories, Kumamoto, Japan). The numbers of migrating cells per field of view were counted on a fluorescent microscope under a 20-fold magnification.

To evaluate the migration activities of human SCLC cells (SBC-5, H1048) and their subclones, they were starved overnight in serum-free MEM. The resultant cells (1×10^5 cells/well) were seeded in the top wells of a 24-well Cell Culture Insert. MEM with 10 % FBS was filled in the bottom wells and incubated for 17 h. The numbers of migrating cells were determined in the same manner described above.

Animals

Male SCID mice, 5–6 weeks old, were obtained from CLEA Japan (Osaka, Japan) and maintained under specific pathogen-free conditions throughout the study. All experiments were performed in accordance with the guidelines established by the Tokushima University Committee on Animal Care and Use.

In vivo metastasis model

To facilitate metastasis formation, SCID mice were pretreated with anti-mouse interleukin-2 receptor β-chain antibody to deplete NK-cells [20, 21]. Two days later, mice were inoculated with SBC-5, H1048, or other transfected clones (1.0×10^6 cells/mouse) into the tail vein. Four weeks (SBC-5 and subclones) or 8 weeks (H1048 and subclones) after tumor cell inoculation, mice were anesthetized by i.p. injection of pentobarbital and X-ray photographs of the mice were taken to determine bone metastasis. Mice were killed humanely under anesthesia, the major organs were removed and weighed, and the number of metastatic colonies on the surface of the organs was counted. The lungs were fixed in Bouin's solution (Sigma, St. Louis, MO) for 24 h. The number of osteolytic lesions on X-ray films was counted by two investigators independently.

Immunohistochemical analyses

For histological analyses, the major organs with metastasis were fixed in 10 % formalin. Frozen tissue sections (8 µm thick) were fixed with cold acetone and used for identification of endothelial cells using rat anti-mouse CD31/PE-CAM-1 antibody (1:250 dilution; BD Biosciences, Cowley, UK) or rat anti-mouse CD68 antibody (1:250 dilution; Abd Serotec, Oxford, UK). To evaluate the microvessel density and tumor-infiltrating macrophages, CD31- and CD68-positive cells in liver metastatic lesions were counted in five random fields per one section at a 400-fold magnification. For the quantification of CD31- and CD68-positive

cells four sections from four mice (total 20 fields) and five sections from five mice (total 25 fields) were analyzed, respectively.

Statistical analysis

The significance of differences in in vitro and in vivo data was analyzed by a one-way ANOVA test. When P values for the overall comparisons were less than 0.05, post hoc pairwise comparisons were performed by a Newman–Keuls Multiple Comparison test. P values of less than 0.05 were considered to be significant. Statistical analyses were performed using the GraphPad Prism program Ver. 4.01.

Results

Generation of cell lines stably overexpressing MSP

First, we sought to establish cell lines which stably overexpressed mouse MSP. Human SCLC, SBC-5 cells were infected with pMIG or pMIG-MSP, and then infected cells were sorted for GFP using flow cytometry. After culturing the initial sorted population, GFP-positive cells comprised more than 85 % of the whole cell population (data not shown). The expression of MSP mRNA and protein was detected in SBC-5-MSP cells, but not in parental SBC-5 cells or SBC-5-Vector cells (Fig. 1a, b).

The culture supernatant of SBC-5-MSP cells, but not that of parental cells or the vector control clone, induced migration of RAW 264.7 (murine macrophage-like cells) and MS1 (murine endothelial cells) (Fig. 2a, b). As expected, both of these cell lines express mouse RON (Fig. 4b), and might be responsive for MSP-mediated migration. These results suggest that MSP secreted by transfectants was biologically active and that it has key roles in infiltration of macrophages and migration of endothelial cells.

MSP gene transduction did not affect the behavior of cancer cells in vitro

We next investigated the effect of MSP gene transduction on in vitro tumor cell behavior related with metastasis. There was no significant difference in cell growth between SBC-5-MSP cells and parental SBC-5 cells or SBC-5-Vector cells (Fig. 3a). Results of the two-chamber migration assay showed that MSP transduction also did not affect cell motility among these three cell lines (Fig. 3b). Willett et al. [22] demonstrated that several lung cancer cell lines expressed both human MSP and human RON, and that human MSP promoted the migration of human RON-expressing cells in an autocrine and/or paracrine manner. Thus, we examined the expression of human RON on

Fig. 1 Evaluation of MSP expression in human SCLC cells. a The expression levels of MSP mRNA in SBC-5 cells and their subclones were determined by RT-PCR, as described in Materials and methods. b The expression levels of MSP protein in SBC-5 cells and their subclones were determined by Western blotting, as desc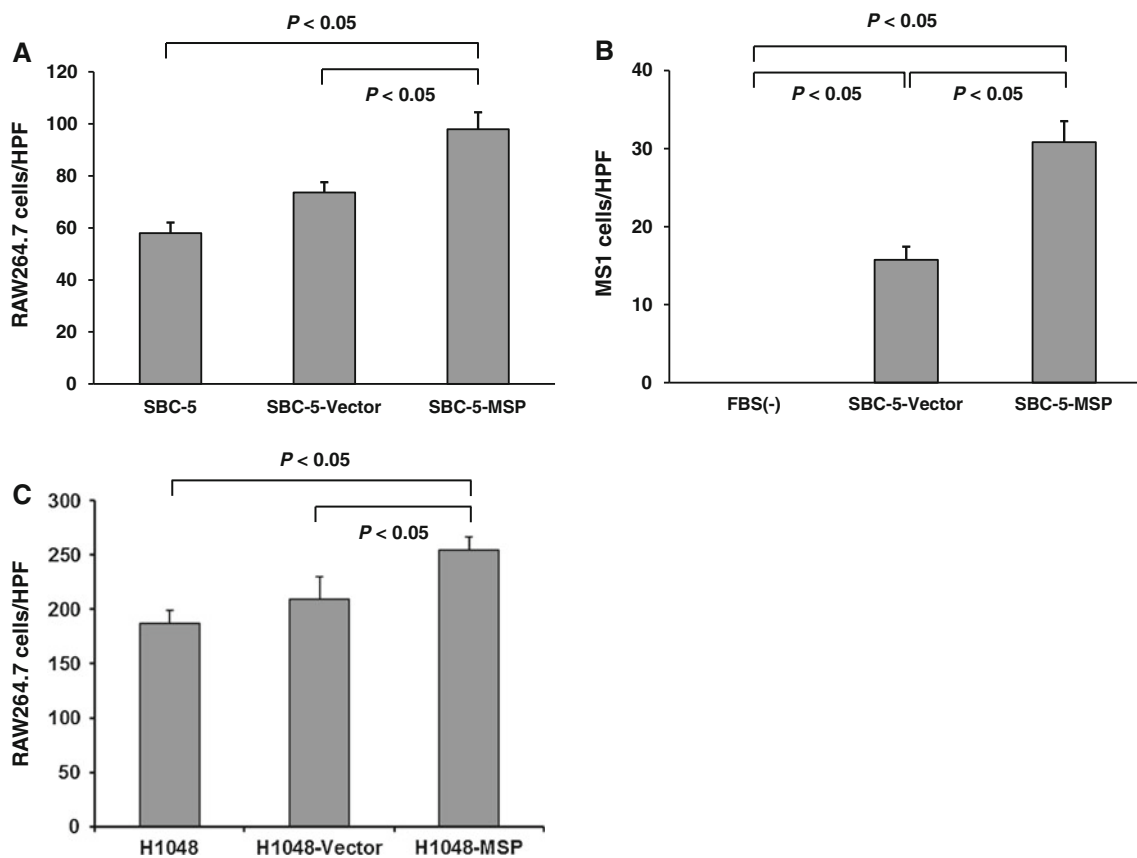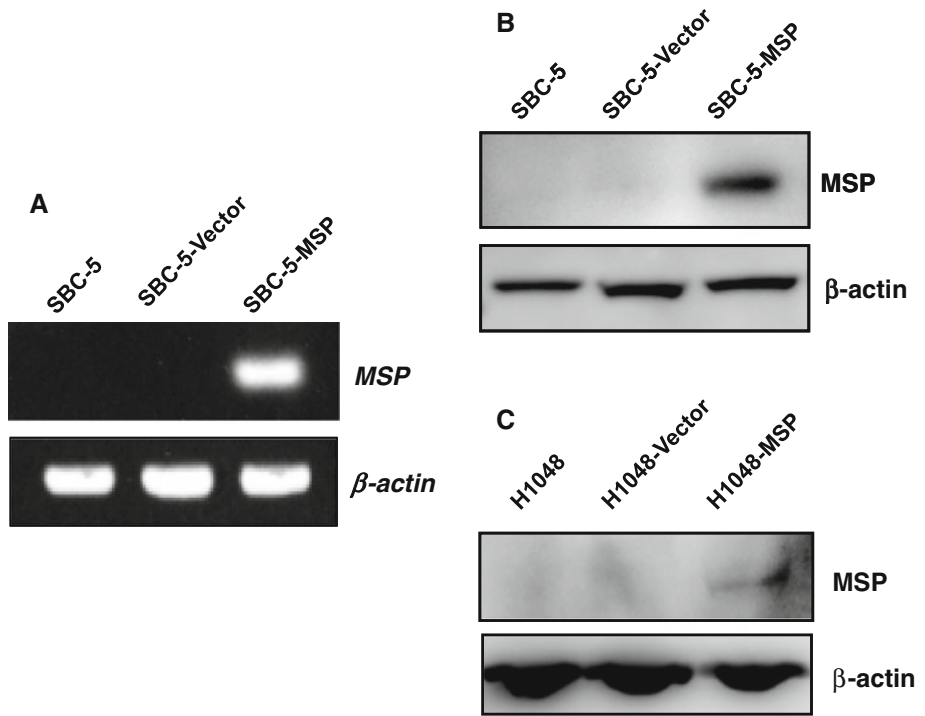ribed in Materials and methods. c The expression levels of MSP protein in H1048 cells and their subclones were determined by Western blotting

Fig. 2 Analysis of the bioactivity of MSP secreted by the MSP transfectant. The bioactivity of MSP, produced by SBC-5-MSP cells, was measured by a two-chamber migration assay. a The culture supernatant of SBC-5-MSP cells, but not that of parental cells or the vector control clone, induced migration of RAW 264.7 cells. b The culture supernatant of SBC-5-MSP cells significantly enhanced the migration of MS1 cells compared with that of SBC-5-Vector cells ($P < 0.05$). c The culture supernatant of H1048-MSP cells, but not that of parental cells or the vector control clone, induced migration of RAW 264.7 cells
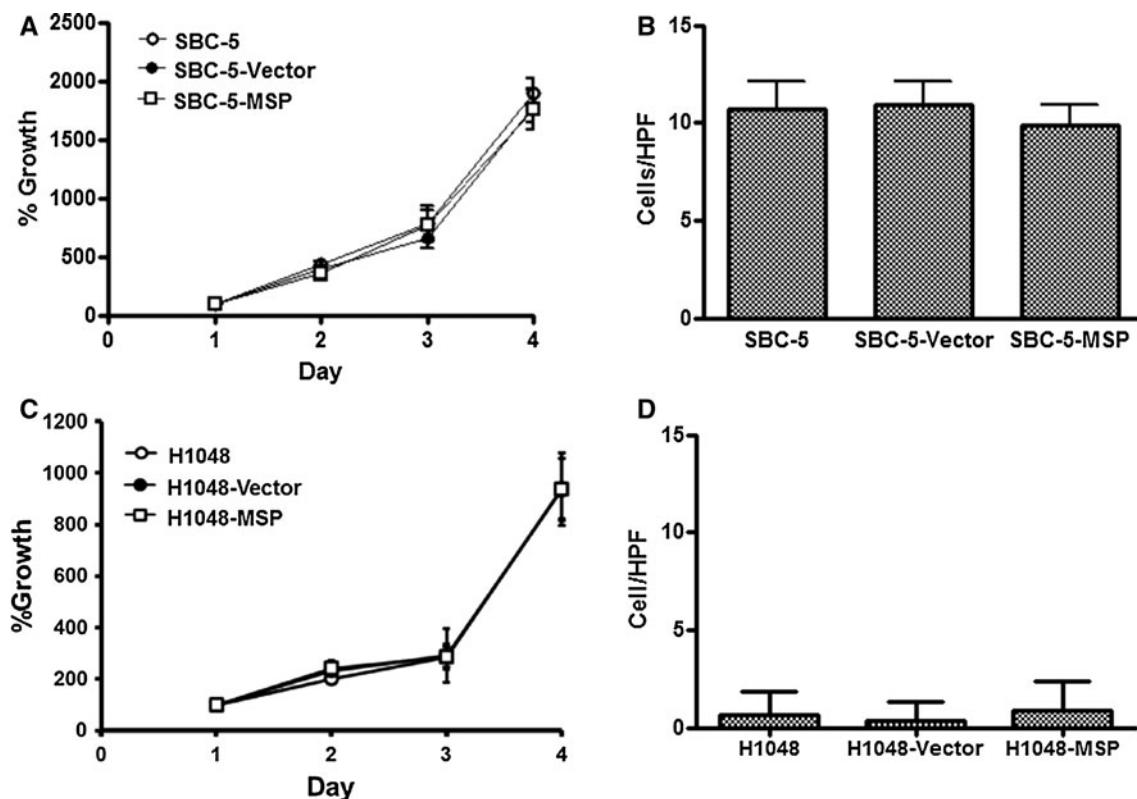
Fig. 3 The effect of MSP gene transduction on in vitro tumor cell behavior. **a** The anchorage-dependent cell growth of SBC-5 cells and their subclones was determined by a MTT assay, as described in Materials and methods. **b** Cell motility of SBC-5 cells and their subclones was determined by a two-chamber migration assay, as described in Materials and methods. **c** The anchorage-dependent cell growth of H1048 cells and their subclones was determined by a MTT assay. **d** Cell motility of H1048 cells and their subclones was determined by a two-chamber migration assay

several human SCLC cell lines, but neither SBC-5 cells nor H1048 cells expressed human RON (Fig. 4a). Since our purpose is to study the effect of MSP to mouse organ microenvironment, we transfected mouse MSP to human cancer cell lines not expressing human RON. Hence, overexpressed mouse MSP was not able to affect cancer cell themselves.

MSP gene transduction resulted in the promotion of experimental liver metastasis in vivo

To evaluate whether MSP signaling could affect cancer metastasis in the presence of the murine microenvironment, we performed in vivo experiments using a previously established model of multiple-organ metastasis in NK-cell depleted SCID mice. In this model, SBC-5 cells produce metastatic colonies predominantly into the liver, lung, and bone [21]. The number of liver metastases was significantly higher in SBC-5-MSP cells than those of parental SBC-5 cells or SBC-5-Vector cells (Table 1; Fig. 5a). There was no statistically significant difference between the numbers of bone and lung metastases among these three cell lines. The expression of MSP mRNA in liver metastatic nodules

produced by SBC-5-MSP cells was confirmed to be maintained (Fig. 5c).

To certify that these effects were not cell-specific, we generated another MSP-overexpressing transfectant, H1048-MSP cells, which were constructed in the same way as SBC-5-MSP (Fig. 1c, 2c). MSP gene transduction did not affect the behavior of H1048-MSP cells in vitro (Fig. 3c, d). H1048 cells also produced metastatic colonies predominantly in the liver, kidney, and bone in NK-cell depleted SCID mice. As with SBC-5-MSP, the number of liver metastases, but not those of kidney and bone metastases, was significantly increased in H1048-MSP cells than those of parental cells or the vector control clone (Table 2; Fig. 5b). These results indicated that MSP has the potential to enhance liver metastases produced by human SCLC cells.

The expression of the factors involved in MSP/RON signaling pathway in normal organs of mice

To elucidate the mechanisms of obvious liver tropism in metastasis formation of MSP-expressing SCLC cells, we examined the expression of the factors involved in MSP/
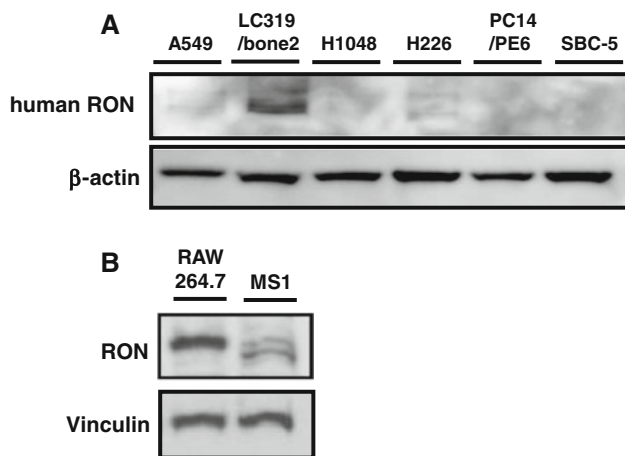
A

B

Fig. 4 The expression of RON in several human lung cancer cells, RAW264.7 and MS1 cells. **a** The expression levels of human RON protein in several lung cancer cells were determined by Western blotting, as described in Materials and methods. **b** The expression levels of mouse RON protein in RAW264.7 and MS1 cells were determined by Western blotting, as described in Materials and methods

RON signaling pathway in normal organs of mice. Then, we found that MSP and HGFA are highly expressed in the liver compared to other organs (Fig. 6a). HGFA is trypsin-like serine proteases, and is known to activate pro-MSP to mature MSP [23], leading to increase mature MSP derived from pro-MSP secreted by tumor cells themselves and/or tumor stroma. Thus, the microenvironment in the liver is favorable for pro-MSP to be translated to activated form. Moreover, RON was phosphorylated in the liver but not in the kidney and the lung, while RON was expressed in all three organs (Fig. 6b), suggesting that the MSP/RON axis was activated in the liver. Taken together, the abundant MSP can affect liver microenvironment and activate MSP/RON axis, which leads to promote liver metastases of MSP-producing SCLC cells.

Microvessel density and tumor-infiltrating macrophages were significantly increased in liver metastatic lesions produced by MSP transfectants

To further explore the mechanism by which MSP enhanced experimental liver metastases, histological analysis was performed using metastatic lesions from the liver by SBC-5, SBC-5-Vector, and SBC-5-MSP cells. For the detection of tumor-associated microvessels and tumor-infiltrating macrophages, we used an anti-mouse CD31 and an anti-mouse CD68 antibody, respectively. Immunohistochemical staining showed that tumor-associated microvessel densities and tumor-infiltrating macrophages were significantly higher in lesions produced by SBC-5-MSP cells, than those produced by parental SBC-5 cells or SBC-5-Vector cells (Fig. 7). These results suggest that MSP secreted from

tumor cells elicited the activation of tumor-infiltrating macrophages and that activated macrophages induced angiogenesis, which may promote liver metastases.

Discussion

Molecular interactions between cancer cells and their microenvironments play crucial roles throughout the multiple steps of metastasis [24, 25]. In this study, we evaluated the interaction of MSP-positive tumor cells with the murine microenvironment using a multiple-organ metastasis model in NK-cell depleted SCID mice. While there was no increase in cell growth or migration in MSP-overexpressing human SCLC cells, MSP overexpression enhanced liver metastases produced by these cells. These findings indicated that MSP may affect organ microenvironments, rather than the tumor cells themselves, to promote metastases.

Tumor-associated macrophage (TAM) infiltration is associated with increased microvessel density, which results in poor prognosis in lung cancer [26]. Moreover, the angiogenic factors secreted by activated macrophages in response to various stimuli in the tumor microenvironment contribute to tumor growth, angiogenesis, and metastasis. In this study, we found that tumor-infiltrating macrophages and microvessel densities were significantly increased in liver metastases by MSP-overexpressing human SCLC cells. These results suggested that MSP secreted from tumor cells elicited chemotaxis and activation of TAMs and that activated TAMs produced angiogenic factors, which could promote angiogenesis and liver metastases. We also demonstrated that the culture supernatant of SBC-5-Vector cells induced migration of murine endothelial cells, and this affects were enhanced by MSP-overexpressing (Fig. 2c). These results indicated that MSP could enhance angiogenesis via a direct effect on endothelial cells in addition to an indirect effect through macrophage activation. Taken together, these data indicate that MSP may be one of the major determinants that affect the properties of tumor stroma and that produce a permissive microenvironment to promote cancer metastasis.

Interestingly, MSP-overexpressing SCLC cells showed liver tropism in metastasis formation. While the number of liver metastases was significantly higher in MSP-overexpressing SCLC cells than those of parental cells or the vector control clone, there were no discernible differences in the numbers of bone and lung metastases among these three cell lines. The reason for these phenomena remains to be elucidated. One possible explanation is that the expression of MSP and HGFA are prominent in the liver compared with other organs (Fig. 6a). MSP and HGFA are primarily produced by hepatocytes and secreted mainly

Table 1 Production of metastasis by SBC-5 cells with or without MSP in NK-cell depleted SCID mice

Cell line	Incidence of metastasis	Liver weight (g)[a]	Number of metastatic colonies[a]		
			Liver	Lung	Bone
SBC-5	6/6	1.3 (1.0–2.2)	70 (50–136)	29 (15–48)	6 (4–8)
SBC-5-Vector	8/8	1.5 (1.2–2.4)	66 (32–133)	26 (8–54)	4 (3–6)
SBC-5-MSP	7/7	1.5 (1.3–1.9)	107 (59–139)[b]	24 (10–47)	5 (3–7)

SBC-5 cells (1 × 106) with or without MSP gene were inoculated intravenously into NK-cell depleted SCID mice on day 0

Mice were killed on day 28 and the formation of metastases was evaluated

Data are representative of five independent experiments with similar results

[a] Values are the means (range) for the indicated numbers of mice

[b] Significantly different from SBC-5 and SBC-5-Vector cells ($P < 0.05$)
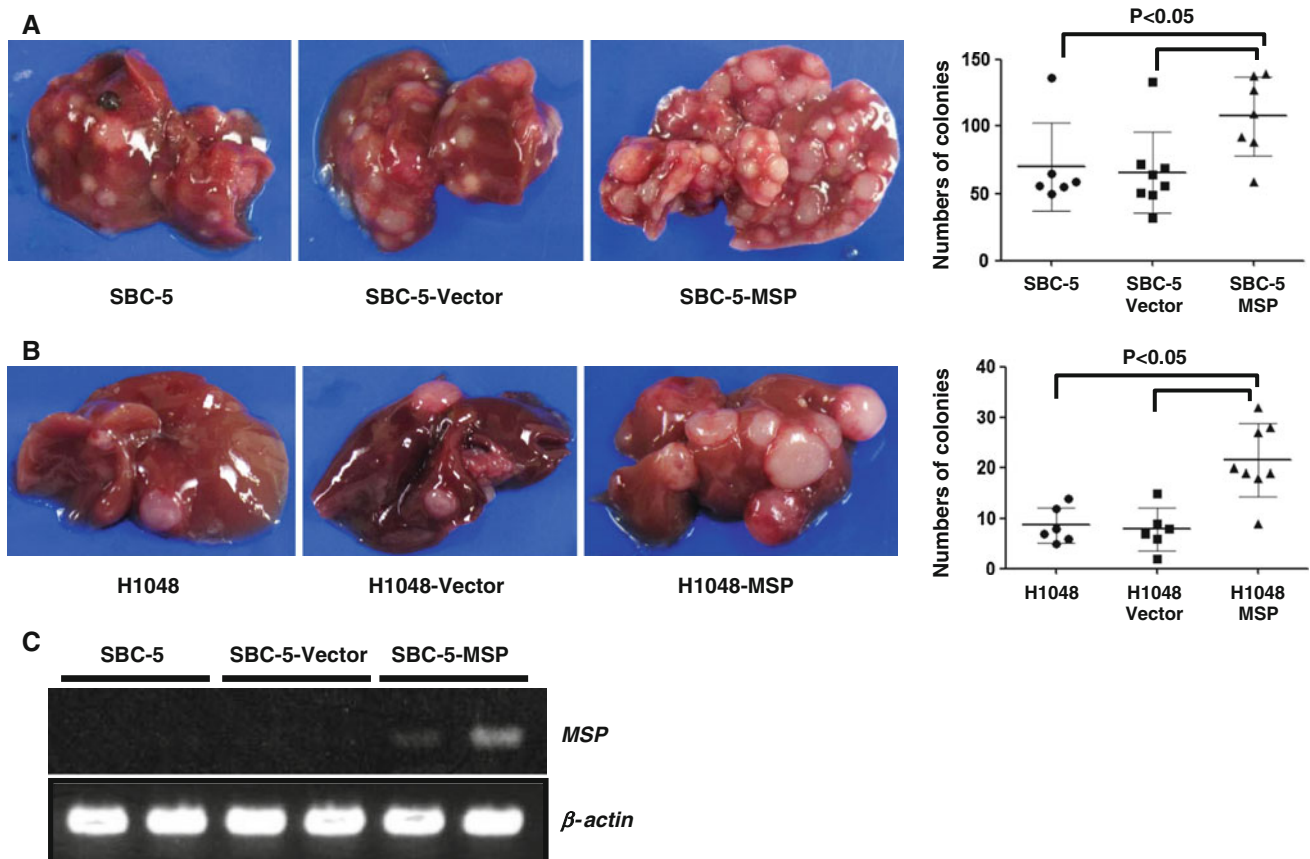

Fig. 5 The effect of MSP gene transduction on experimental liver metastasis formation produced by human SCLC cells. **a** The experimental liver metastases by SBC-5-MSP cells significantly increased compared with SBC-5 and SBC-5-Vector cells. Representative photographs of the liver (*left panel*) and the numbers of liver metastatic colonies in each experimental group (*right panel*) are shown. **b** The experimental liver metastases by H1048-MSP cells significantly increased compared with H1048 and H1048-Vector cells. Representative photographs of the liver (*left panel*) and the numbers of liver metastatic colonies in each experimental group (*right panel*) are shown. **c** The expression levels of MSP mRNA in metastatic liver lesions by SBC-5 cells and their subclones were determined by RT-PCR, as described in Materials and methods

from the liver [27, 28]. RON mRNA and protein are also expressed in the normal liver, and its expression is localized to hepatocytes and Kupffer cells, the resident macrophage population of the liver [27]. These facts means that liver have the most advanced environment used to convert pro-

MSP to mature form, and are susceptible organs by pro-MSP secreted from cancer cells. Therefore, in liver metastatic lesions, MSP which was secreted by tumor cells may induce RON activation in hepatocytes and Kupffer cells, which may produce permissive organ microenvironments for the

Table 2 Production of metastasis by H1048 cells with or without MSP in NK-cell depleted SCID mice

Cell line	Incidence of metastasis	Liver weight (g)[a]	Number of metastatic colonies[a]		
			Liver	Lung	Bone
H1048	6/6	0.9 (0.6–1.1)	9 (5–14)	24 (11–30)	3 (1–5)
H1048-Vector	6/6	1.0 (0.7–1.5)	8 (2–15)	31 (19–36)	5 (3–6)
H1048-MSP	8/8	1.2 (0.8–1.5)	22 (9–32)[b]	29 (15–43)	3 (1–6)

H1048 cells (1×10^6) with or without MSP gene were inoculated intravenously into NK-cell depleted SCID mice on day 0

Mice were killed on day 56 and the formation of metastases was evaluated

Data are representative of five independent experiments with similar results

[a] Values are the means (range) for the indicated numbers of mice

[b] Significantly different from H1048 and H1048-Vector cells ($P < 0.05$)
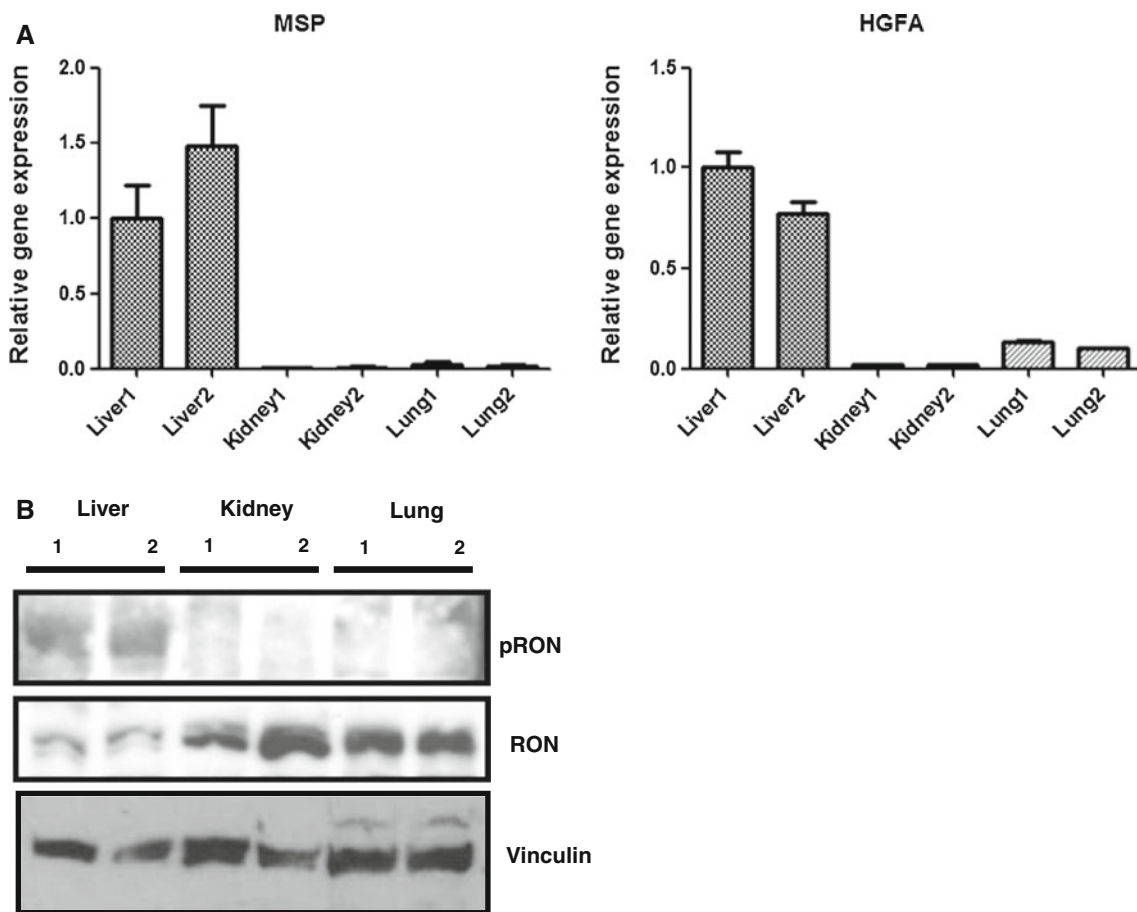

Fig. 6 The expression of the factors involved in MSP/RON signaling pathway in normal organs of mice. **a** The expression levels of MSP and HGFA mRNA in the liver, the kidney and the lung of mice were determined by quantitative PCR, as described in Materials and methods. **b** The expression levels of RON and pRON protein in the liver, the kidney and the lung of mice were determined by Western blotting, as described in Materials and methods

promotion of tumor growth. Another explanation is that angiogenesis is more important for metastasis formation in the liver than other organs. Indeed, disease-free and overall survival of metastatic liver cancer was reported to be closely associated with the number of microvessels in the tumor [29], and the liver parenchyma adjacent to synchronous liver metastases provides an angiogenic prosperous environment for metastatic tumor growth in the presence of the primary tumor [30]. Moreover, we recently reported that angiogenesis is hardly involved in experimental bone metastasis formation by SBC-5 cells [31]. Further studies are warranted to ascertain the precise mechanisms for liver tropism in
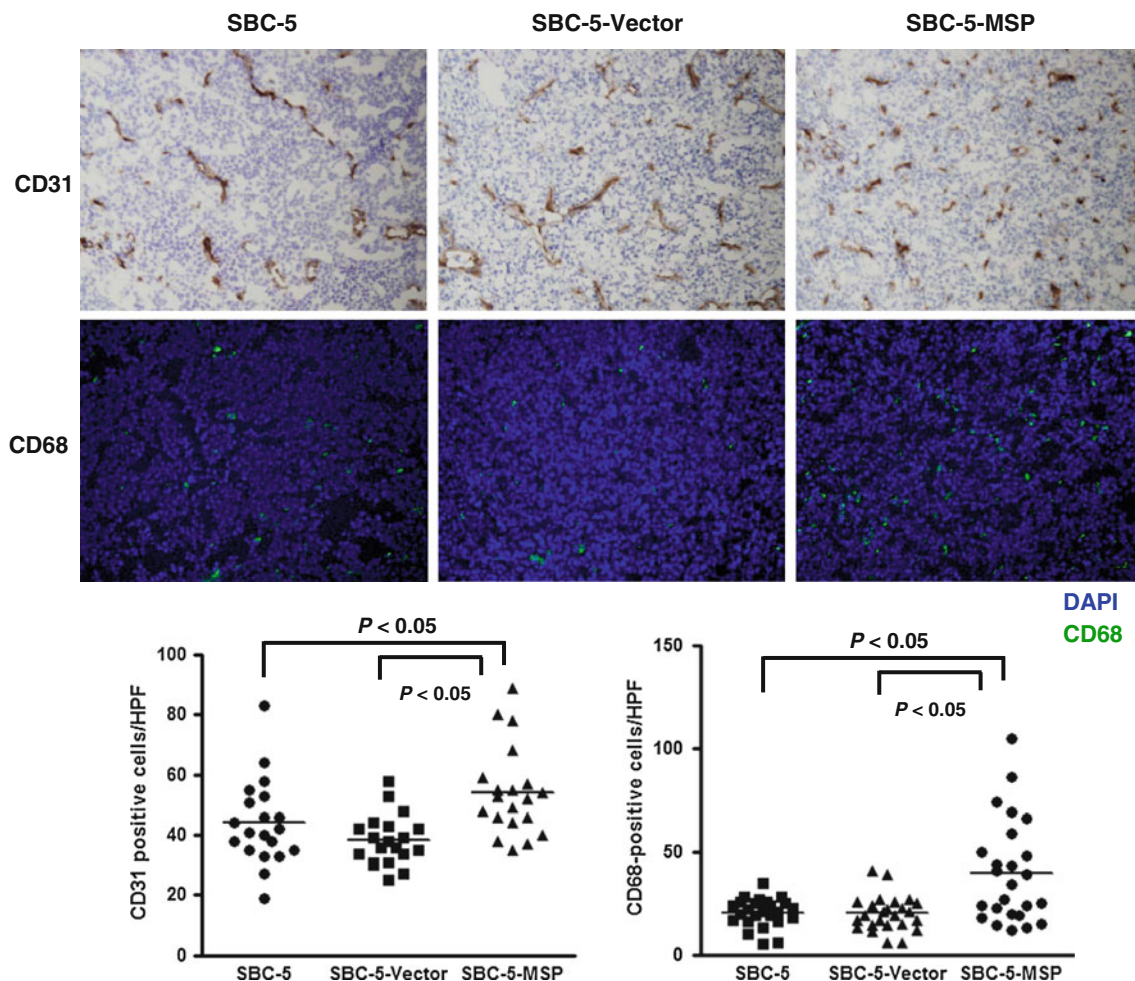
Fig. 7 Analyses of the microvessel density and tumor-infiltrating macrophages in liver metastatic lesions produced by SBC-5 cells transfected with or without the MSP gene. Immunohistochemical staining of the liver was performed as described in Materials and methods. The amount of vascularization determined by CD31 staining and macrophages by CD68 staining were significantly increased in SBC-5-MSP tumors than those of SBC-5 and SBC-5-Vector tumors. *$P < 0.05$ in comparison to SBC-5 tumors and SBC-5-Vector tumors

metastasis formation observed in MSP-overexpressing SCLC cells.

Accumulating evidence indicates that activation of the MSP/RON axis affected the ability of tumor cells themselves to migrate, invade, and/or grow in distant tissues [11–13]. For example, the overexpression of MSP facilitated metastases to various organs, especially to bone, produced by mammary tumors in transgenic mice [12]. Constitutive expression of RON was shown to induce epithelial mesenchymal transition, marked by phenotypic changes and alterations in cell motility [32], and was correlated with reduced disease-free survival of breast cancer patients [33]. In lung cancer, MSP and its receptor, RON, were also overexpressed in 25–44 % and 62–72 % of tumors, respectively [22, 34]. In vitro tests of RON activity in certain lung cancer cell lines demonstrated that MSP stimulation induced RON phosphorylation and increased cell motility in an autocrine and/or paracrine manner [22].

Furthermore, MSP expression was up-regulated in bone metastatic lesions by SCLC cells [13]. These observations suggested that MSP may affect not only tumor microenvironments but also the tumor cells themselves to promote the progression and metastases of lung cancer. While there are no clinical reports about MSP expression in SCLC, recent evidence has demonstrated that the frequency and intensity of RON expression was much higher in lung tumors of neuroendocrine origin such as SCLC and in secondary tumors which metastasized to the brain [34]. These findings also suggest the importance of MSP/RON axis to interact with organ microenvironment and promote distant metastases of SCLC cells.

Recently, a humanized monoclonal antibody, IMC-41A10, that blocks the interaction of RON with MSP has been developed. IMC-41A10 not only inhibits the binding of MSP to RON, but also diminishes RON phosphorylation and its downstream signaling. In addition, IMC-41A10 also

significantly decreased tumor growth of murine xenografts from various subcutaneously injected cancer cell lines, including lung cancer [35]. These results highlight the potential therapeutic usefulness of MSP/RON axis inhibition in human cancers.

In conclusion, we showed that MSP gene transduction resulted in the facilitation of experimental liver metastases via the promotion of angiogenesis in NK-cell depleted SCID mice by human SCLC cells. The capability of MSP to modify organ microenvironments may uncover a unique and effective strategy to inhibit liver metastases of SCLC in humans.

References

1. Sone S, Yano S (2007) Molecular pathogenesis and its therapeutic modalities of lung cancer metastasis to bone. Cancer Metastasis Rev 26:685–689

2. Skeel A, Yoshimura T, Showalter SD, Tanaka S, Appella E, Leonard EJ (1991) Macrophage stimulating protein: purification, partial amino acid sequence, and cellular activity. J Exp Med 173:1227–1234

3. Bezerra JA, Witte DP, Aronow BJ, Degen SJ (1993) Hepatocyte-specific expression of the mouse hepatocyte growth factor-like protein. Hepatology 18:394–399

4. Yoshimura T, Yuhki N, Wang MH, Skeel A, Leonard EJ (1993) Cloning, sequencing, and expression of human macrophage stimulating protein (MSP, MST1) confirms MSP as a member of the family of kringle proteins and locates the MSP gene on chromosome 3. J Biol Chem 268:15461–15468

5. Wang MH, Skeel A, Leonard EJ (1996) Proteolytic cleavage and activation of pro-macrophage-stimulating protein by resident peritoneal macrophage membrane proteases. J Clin Invest 97:720–727

6. Nanney LB, Skeel A, Luan J, Polis S, Richmond A, Wang MH, Leonard EJ (1998) Proteolytic cleavage and activation of pro-macrophage-stimulating protein and upregulation of its receptor in tissue injury. J Invest Dermatol 111:573–581

7. Ronsin C, Muscatelli F, Mattei MG, Breathnach R (1993) A novel putative receptor protein tyrosine kinase of the met family. Oncogene 8:1195–1202

8. Gaudino G, Follenzi A, Naldini L, Collesi C, Santoro M, Gallo KA, Godowski PJ, Comoglio PM (1994) RON is a heterodimeric tyrosine kinase receptor activated by the HGF homologue MSP. EMBO J 13:3524–3532

9. Iwama A, Yamaguchi N, Suda T (1996) STK/RON receptor tyrosine kinase mediates both apoptotic and growth signals via the multifunctional docking site conserved among the HGF receptor family. EMBO J 15:5866–5875

10. Peace BE, Hughes MJ, Degen SJ, Waltz SE (2001) Point mutations and overexpression of Ron induce transformation, tumor formation, and metastasis. Oncogene 20:6142–6151

11. Kretschmann KL, Eyob H, Buys SS, Welm AL (2010) The macrophage stimulating protein/Ron pathway as a potential therapeutic target to impede multiple mechanisms involved in breast cancer progression. Curr Drug Targets 11:1157–1168

12. Welm AL, Sneddon JB, Taylor C, Nuyten DS, van de Vijver MJ, Hasegawa BH, Bishop JM (2007) The macrophage-stimulating protein pathway promotes metastasis in a mouse model for breast cancer and predicts poor prognosis in humans. Proc Natl Acad Sci U S A 104:7570–7575

13. Kakiuchi S, Daigo Y, Tsunoda T, Yano S, Sone S, Nakamura Y (2003) Genome-wide analysis of organ-preferential metastasis of human small cell lung cancer in mice. Mol Cancer Res 1:485–499

14. Kiura K, Watarai S, Shibayama T, Ohnoshi T, Kimura I, Yasuda T (1993) Inhibitory effects of cholera toxin on in vitro growth of human lung cancer cell lines. Anticancer Drug Des 8:417–428

15. Otsuka S, Hanibuchi M, Ikuta K, Yano S, Goto H, Ogino H, Yamada T, Kakiuchi S, Nishioka Y, Takahashi T, Sone S (2009) A bone metastasis model with osteolytic and osteoblastic properties of human lung cancer ACC-LC-319/bone2 in natural killer cell-depleted severe combined immunodeficient mice. Oncol Res 17:581–591

16. Morita S, Kojima T, Kitamura T (2000) Plat-E: an efficient and stable system for transient packaging of retroviruses. Gene Ther 7:1063–1066

17. Tanaka T, Kitamura F, Nagasaka Y, Kuida K, Suwa H, Miyasaka M (1993) Selective long-term elimination of natural killer cells in vivo by an anti-interleukin-2 receptor β chain monoclonal antibody in mice. J Exp Med 178:1103–1107

18. Yano S, Zhang H, Hanibuchi M, Miki T, Goto H, Uehara H, Sone S (2003) Combined therapy with a new bisphosphonate, minodronate (YM529), and chemotherapy for multiple organ metastases of small cell lung cancer cells in severe combined immunodeficient mice. Clin Cancer Res 9:5380–5385

19. Green LM, Reade JL, Ware CF (1984) Rapid colometric assay for cell viability: application to the quantitation of cytotoxic and growth inhibitory lymphokines. J Immunol Methods 70:257–268

20. Yano S, Nishioka Y, Izumi K, Tsuruo T, Tanaka T, Miyasaka M, Sone S (1996) Novel metastasis model of human lung cancer in SCID mice depleted of NK cells. Int J Cancer 67:211–217

21. Miki T, Yano S, Hanibuchi M, Sone S (2000) Bone metastasis model with multiorgan dissemination of human small-cell lung cancer (SBC-5) cells in natural killer cell-depleted SCID mice. Oncol Res 12:209–217

22. Willett CG, Wang MH, Emanuel RL, Graham SA, Smith DI, Shridhar V, Sugarbaker DJ, Sunday ME (1998) Macrophage-stimulating protein and its receptor in non-small-cell lung tumors: induction of receptor tyrosine phosphorylation and cell migration. Am J Respir Cell Mol Biol 18:489–496

23. Kawaguchi M, Orikawa H, Baba T, Fukushima T, Kataoka H (2009) Hepatocyte growth factor activator is a serum activator of single-chain precursor macrophage-stimulating protein. FEBS J 13:3481–3490

24. Liotta LA, Kohn EC (2001) The microenvironment of the tumor-host interface. Nature 411:375–379

25. Fidler IJ (2002) The organ microenvironment and cancer metastasis. Differentiation 70:498–505

26. Takanami I, Takeuchi K, Kodaira S (1999) Tumor-associated macrophage infiltration in pulmonary adenocarcinoma: association with angiogenesis and poor prognosis. Oncology 57:138–142

27. Wagh PK, Peace BE, Waltz SE (2008) Met-related receptor tyrosine kinase Ron in tumor growth and metastasis. Adv Cancer Res 100:1–33

28. Iida I, Johkura K, Teng R, Kubota S, Cui L, Zhao X, Ogiwara N, Okouchi Y, Asanuma K, Nakayama J, Sasaki K (2003) Immunohistochemical localization of hepatocyte growth factor activator (HGFA) in developing mouse liver tissues. Heterogeneous

distribution of HGFA protein. J Histochem Cytochem 9:1139–1149

29. Nanashima A, Shibata K, Nakayama T, Tobinaga S, Araki M, Kunizaki M, Takeshita H, Hidaka S, Sawai T, Nagayasu T, Yasutake T (2009) Clinical significance of microvessel count in patients with metastatic liver cancer originating from colorectal carcinoma. Ann Surg Oncol 16:2130–2137

30. van der Wal GE, Gouw AS, Kamps JA, Moorlag HE, Bulthuis ML, Molema G, de Jong KP (2012) Angiogenesis in synchronous and metachronous colorectal liver metastases: the liver as a permissive soil. Ann Surg 255:86–94

31. Gabr AG, Goto H, Hanibuchi M, Ogawa H, Kuramoto T, Suzuki M, Saijo A, Kakiuchi S, Trung VT, Sakaguchi S, Moriya Y, Sone S, Nishioka Y (2012) Erlotinib prevents experimental metastases of human small cell lung cancer cells with no epidermal growth factor receptor expression. Clin Exp Metastasis (in press)

32. Wang D, Shen Q, Chen YQ, Wang MH (2004) Collaborative activities of macrophage-stimulating protein and transforming growth factor-β1 in induction of epithelial to mesenchymal transition: roles of the RON receptor tyrosine kinase. Oncogene 23:1668–1680

33. Lee WY, Chen HH, Chow NH, Su WC, Lin PW, Guo HR (2005) Prognostic significance of co-expression of RON and MET receptors in node-negative breast cancer patients. Clin Cancer Res 11:2222–2228

34. Kanteti R, Krishnaswamy S, Catenacci D, Tan YH, El-Hashani E, Cervantes G, Husain AN, Tretiakova M, Vokes EE, Huet H, Salgia R (2012) Differential expression of RON in small and non-small cell lung cancers. Genes Chromosomes Cancer 51:841–851

35. O'Toole JM, Rabenau KE, Burns K, Lu D, Mangalampalli V, Balderes P, Covino N, Bassi R, Prewett M, Gottfredsen KJ, Thobe MN, Cheng Y, Li Y, Hicklin DJ, Zhu Z, Waltz SE, Hayman MJ, Ludwig DL, Pereira DS (2006) Therapeutic implications of a human neutralizing antibody to the macrophage-stimulating protein receptor tyrosine kinase (RON), a c-MET family member. Cancer Res 66:9162–9170